

Envelope Tracking Amplification with Reduced Slew-Rate and Bandwidth Envelopes

Pedro P. Vizarreta⁽¹⁾, Gabriel Montoro⁽¹⁾, Pere L. Gilabert⁽¹⁾, Eduard Bertran⁽¹⁾,
Jordi Berenguer⁽¹⁾, Antoni Gelonch⁽¹⁾, José Ángel García⁽²⁾

[pvizarreta, montoro, plgilabert, bertran, berenguer, antoni] @tsc.upc.edu, joseangel.garcia@unican.es

⁽¹⁾Department of Signal Theory and Communications, Universitat Politècnica de Catalunya (UPC)

Esteve Terradas, 7 - 08860 Castelldefels, Barcelona, Spain

⁽²⁾Communication Engineering Department, Universidad de Cantabria, Plaza de la Ciencia, 39005, Santander, Spain

Abstract—This paper presents an Envelope Tracking Power Amplifier whose architecture includes a Hybrid Envelope Amplifier (HEA) and an algorithm to adapt the envelope's characteristics to the HEA's limitations. The HEA attempts to combine the high efficiency of a switched amplifier with the wide band capabilities of a linear amplifier. A modified Slew Rate (SR) reduction algorithm cope with the bandwidth and SR limitations of the HEA. On the other hand, the non-linearities introduced by this Envelope Amplifier (EA) and by the dynamic supply are compensated using Digital Pre-Distortion. Results show that these non-linearities are compensable and that the architecture offers higher efficiency figures compared to the conventional linear EA.

I. INTRODUCTION

Architectures based on dynamic power supply, such as the Envelope Tracking (ET) and Envelope Elimination and Restoration (EER), are currently actively investigated as possible solutions to achieve simultaneously linear and high efficient amplification. Although many studies have been carried out in these architectures, their main limitation still lies on the Envelope Amplifier (EA) which is required to be highly linear and efficient in a wide band range.

Because most of the envelope's energy is concentrated in its low frequency components, such portion can be efficiently amplified using switched amplifiers while the remaining portion of the spectrum can be amplified using a linear amplifier. Such principle, called Bandwidth (BW) splitting, was firstly introduced by Raab in [1] and have been recently used in an EA for EER architectures in [2]. Following this principle the HEA splits the spectrum of the envelope and amplifies the low frequencies using a Switched Envelope Amplifier (SEA) while the high frequencies are amplified by a Linear Envelope Amplifier (LEA). Although the most efficient strategy for the RFPA is to supply it with the envelope of the RF signal, it is not always possible due to the large BW exhibited by this signal. Nevertheless, in such cases is possible to use techniques based on Slew Rate (SR) [3] and BW [4] reduction to relax the EA's requirements at the expense of efficiency degradation.

This paper presents an ET architecture incorporating a HEA. An algorithm for real-time envelope's BW and SR reduction has been included to maintain the envelope's spectrum within the limits of the LEA's frequency response. The frequency splitting of the reduced envelope is performed digitally as

well as the compensation of its nonlinear distortions. Slow Envelope Dependent Digital Pre-Distortion (SED-DPD) is used to compensate separately the distortions introduced by the dynamic power supply. The rest of this paper is organized as follows. Section II is devoted to the envelope reduction algorithm, its effects over the ET efficiency and the modifications carried out over the original version of the algorithm. Section III describes the experimental set-up used to evaluate the performance of the proposed architecture and describes both the behavioral models and the DPD structure for the RFPA as well as for the HEA. Sections IV and V describe the experimental results and conclusions respectively.

II. ENVELOPE REDUCTION ALGORITHM

There exist two different approaches in the literature to adapt the envelope characteristics to the EA limitations. These approaches modify the envelope to obtain either a SR [3] or a BW [4] reduced version of it. As a counterpart, in both cases the resulting signal produces a small back-off on the RFPA reducing its drain efficiency. In fact, its drain efficiency decays as the SR and BW restriction increases. Fig. 1 shows the efficiency degradation when considering different levels of SR and BW reduction. The measurements presented in Fig. 1 were obtained using the algorithm presented in [3]. The parameter N which is related to the maximum allowed increment in the signal's slope, is swept in order to change the SR and BW reduction level. Notice that the drain efficiency decays more or less linearly with the BW reduction, while decays logarithmically with the SR reduction, as it was theoretically predicted in [3].

Although Fig. 1 evidences that there is a relationship between the SR and the BW reduction, there is not a clear limitation of the BW of the resulting signal when using the algorithm presented in [3] making challenging its amplification if only switched methods are considered. On the other hand, the method proposed in [4] limits the BW of the envelope using an iterative algorithm which is advantageous for switched amplifiers but representing an issue for real time applications. Therefore, the algorithm for envelope reduction used in this paper is based on the one proposed in [1] and includes modifications over its original version to restrict not only the SR but also the BW of the resulting signal.

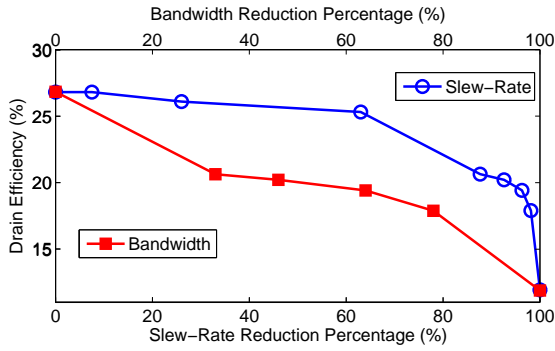


Fig. 1. SR and BW reduction vs efficiency .

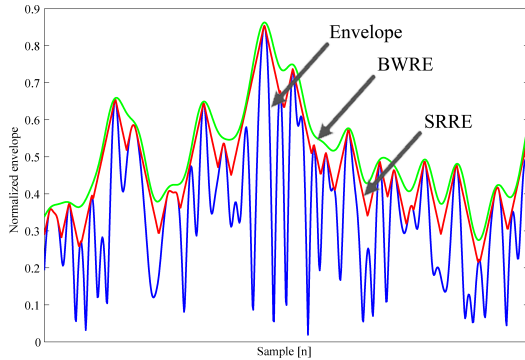


Fig. 2. Time representation of the envelope and its SR and BW limited.

Fig. 2 and Fig. 3 show the time and spectral representation of a 64-QAM signal's envelope in blue, its SR Reduced Envelope (SRRE) in red and its BW Reduced Envelope (BWRE) in green. From the waveform of the SRRE can be deduced that the lack of BW limitation is mainly due to the presence of peaks. Those peaks are introduced by the algorithm when it is necessary to change drastically from a positive to a negative slope (convex peak), or vice-versa (concave peak). Therefore, the modifications performed over this algorithm were focus on their elimination.

The peaks suppression is performed while the signal is being processed by the algorithm. When a convex peak is generated, its maximum value is replicated N -times. This replication process only takes place if that value is above its neighbor values. Afterwards, to remove the introduced discontinuities, the signal is averaged using $N/2$ samples before the peak location and $N/2$ samples after the peak location. The replication of the local maximums ensures that all the maximums are preserved even after the averaging process. The number of samples, N , is chosen according with the desired bandwidth of the output signal. For example, if the samples are generated at time-intervals T_s , then N is giving by $N = 1/BW/T_s$. This process leads to a free-peak and BW limited signal, as shown the green signal in Fig. 2 and Fig. 3. It is worth to mention that after the averaging process, high-frequency components could still

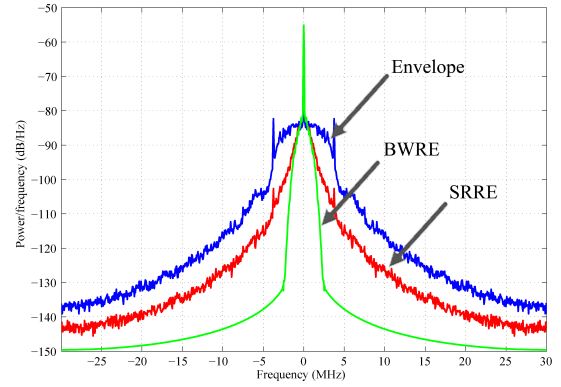


Fig. 3. Frequency representation of the envelope and its SR and BW limited.

be present and can be removed by low-pass filtering. Special attention should be paid on the final filtering process, since the passing band should be wider or equal to the equivalent low-pass filter performed by the averaging process. As counterpart, the modifications over the original algorithm reduce even more the efficiency of the ET PA since the BW reduced envelope is always above the SR reduced envelope.

The modified algorithm is suitable to be implement in digital processors due to its simplicity. The results shown in Fig. 2 and Fig. 3 were extracted from its implementation on a Field Programmable Gate Array (FPGA) Virtex-4 whose clock speed was set to 60 MHz.

III. EXPERIMENTAL SET-UP

Fig. 4 shows the experimental set-up of the proposed ET architecture. The envelope of the generated signal is reduced in SR and BW to ensure that the spectral characteristics of the signal are within the LEA's limitations. Afterwards, a digital split-band is performed accordingly with the available hardware features. The high frequency components go through the LEA while the low frequencies are first modulated using Pulse Width Modulation (Delta-Sigma modulation or any other pulse codification are also possible), then amplified by the SEA and low pass filtered. Both frequency components are proportionally amplified and later combined using a bias-tee, whose L and C are chosen according to the cutoff frequency.

The SEA was realized using the Supertex Integrated Circuits (IC) MD1211 and TC6320 followed by a 8th order passive Low Pass Filter (LPF). The LEA consists on the high-speed (35MHz BW and 900V/ μ s SR At $A_v=2$ and 10 Ω load) high-current (1.1 A) Linear Technology IC LT1210. The HEA supplies dynamically the voltage to a Cree Inc. Eval. Board CGH40006P-TB (GaN transistor) to amplify a 64-QAM signal generated by an Agilent MXG N5182A RF vector signal generator. The RF vector signal generator modulates the signal at 2 GHz while the envelopes are generated by a Tabor WW2572A arbitrary wave generator.

The RF output signal and the RFPAs supply voltage are monitored by an Agilent Infinium DSO90404A oscilloscope

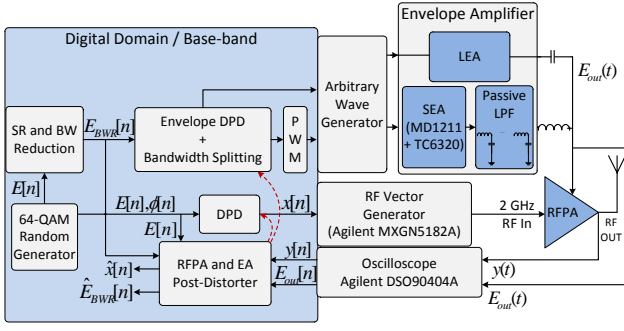


Fig. 4. Block-diagram of the experimental ET set-up.

to later estimate the RFPA and EA distortions respectively. The DPD is performed in both cases following the indirect learning method. In the case of the RFPA DPD, a SED-DPD compensates the distortion caused by using a power supply different to the RF-input's envelope. The overall system was connected to, and controlled by, a PC running MATLAB.

A. RFPA model and DPD

In ET architectures, the nonlinear distortion that appears at the RFPA's output when is supplied by a signal different to the envelope cannot be compensated only using dynamic behavioral . Instead, the model needs to take into account the RFPA's supply signal to compensate this type of nonlinear distortion [5]. Moreover, when the RF-signal exhibits significant bandwidth and rapid envelope variations the memory effects of the PA have to be taken into account as well. Therefore, taking into account the notation described in Fig. 4, and according to [5], in the digital domain the PA Input-Output (I/O) relationship can be described as follows:

$$y[n] = \sum_{i=0}^M \sum_{j=0}^N \sum_{p=0}^P \sum_{q=0}^Q \gamma_{ijpq} x[n - \tau_j] |x[n - \tau_j]|^i (E_{out}[n - \tau_q])^p \quad (1)$$

where $E_{out}[n]$ is a BW-reduced version of the original envelope, which is assumed to be equal to the generated signal, $E_{BWR}[n]$. $E_{out}[n]$ provides the power supply to the RFPA while $x[n]$ and $y[n]$ are its input and output signals respectively. On the other hand, τ_j and τ_q (with $\tau_0 = 0$) are the most significant tap delays of the reduced envelope and input signal that contribute to characterize the memory effects.

The mathematical model described in (1) is also used to perform the SED-DPD following the indirect learning method. Least squares fitting approach is used to estimate the post-distorter function from the input and output RFPA measured data. Fig. 5 shows in red the distortion occasioned in the AM-AM characteristic when the SR reduced envelope supplies the RFPA. Fig. 5 also shows in blue the AM-AM characteristic after applying the SED-DPD

B. Envelope Amplifier model and DPD

In order maintain the efficiency of the whole ET architecture, the EA should operate at its maximum efficiency.

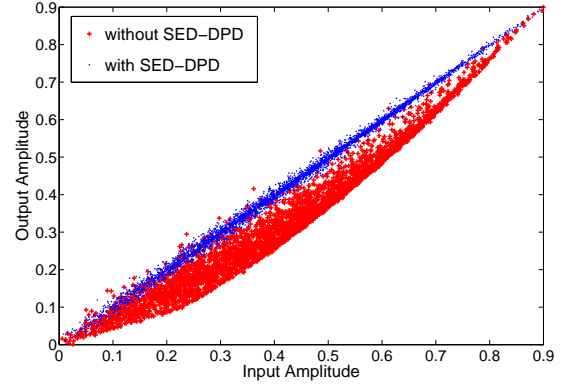


Fig. 5. AM-AM of an ET PA with the slow envelope (N=30).

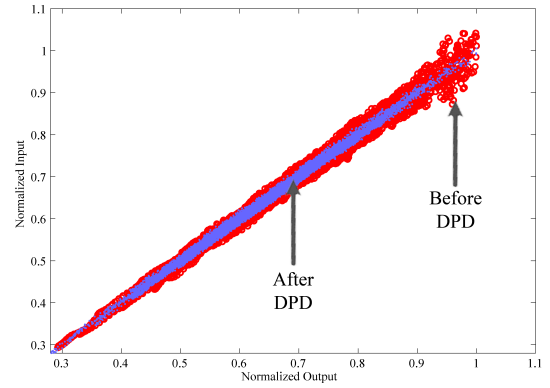


Fig. 6. AM-AM characteristic of the HEA.

Therefore, the LEA should be kept close to the saturation point where nonlinearities arise. Moreover, additional nonlinearities appear because of the interaction of inductors and capacitors directly with the RF signal. Those distortions appear at the EA's output as clipping on the signal's maximums and ripple resembling the envelope of the RF input signal.

The EA's I/O relationship can be described using a polynomial structure. Following the notation used in Fig. 4 such relationship, in the digital domain, could be written as follows:

$$E_{out}[n] = \sum_{i=0}^M \sum_{j=0}^N \sum_{p=0}^P \sum_{q=0}^Q \gamma_{ijpq} |x[n - \tau_j]|^i (E_{BWR}[n - \tau_q])^p \quad (2)$$

Following a similar procedure to the described on the RFPA's DPD, (2) is used to perform the DPD of the envelope.

Fig. 6 shows the AM-AM characteristic of the HEA. The dots displayed in red and blue show the input-output relationship before and after performing DPD. Notice that the largest the amplitude is the bigger the distortion is. Moreover, there is a notable distortion for the largest amplitudes even when there is no obvious evidence of the LEA compression point.

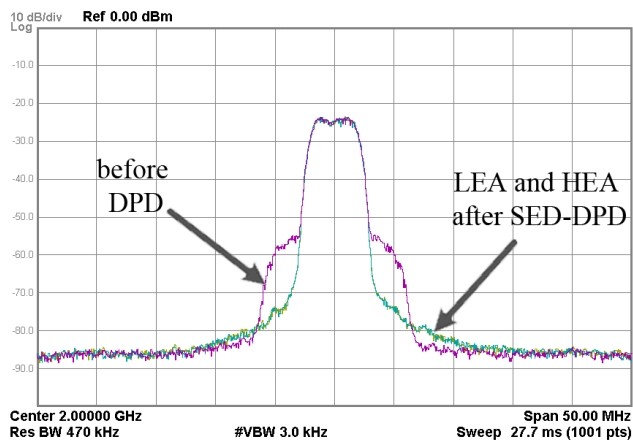


Fig. 7. Spectrum of a 64-QAM signal before and after SED-DPD .

IV. EXPERIMENTAL RESULTS

For comparative purposes, measurements were performed using a 64-QAM, 4.5 MHz BW. Its envelope's BW was considered to extend up to 30 MHz and therefore suitable to amplify with the LEA included in the set-up. Fig. 7 shows the spectrum of the 64-QAM signal before and after the SED-DPD. As can be observed, using the LEA as well as using the HEA the spectral regrowth associated to the EA and RFPA nonlinear behavior has been corrected.

Four cases, based on two main scenarios, are studied to evaluate the performance of the proposed ET architecture. In the first scenario, the RFPA's supply ($V_{DD}(t)$) is the envelope of its input ($E(t)$) which leads to two cases of study: when the EA is the LEA and when the EA is the HEA. In the second scenario, ($V_{DD}(t)$) is the BW Reduced Envelope signal ($E_{BWR}(t)$) which leads also to two cases of study: when the EA is the LEA and when the EA is the HEA. In all these cases the performance comparisons of the proposed ET were realized after compensating the inherent nonlinear distortions.

Table I summarizes the measurements results. Because the scope of this paper is to evaluate the efficiency of the proposed architecture, the SEA's efficiency is assumed to be 90%, which is a reasonable figure for a switched DC-DC converter providing the output power range presented in this study. It is outstanding in Table I the efficiency enhancement of both the LEA (η_{LEA}) and the EA (η_{EA}) when using the HEA. Moreover, the EA's efficiency is higher when the envelopes' BW reduction is performed (77% for $V_{DD}(t) = E(t)$ and 83% for $V_{DD}(t) = E_{BWR}(t)$). As expected, there is an efficiency reduction on the ET architecture (η_{ET}) when the BWRE is used to supply the RFPA.

Besides the efficiency improvements, the linearity levels are kept relatively high. Thanks to the DPD, the EVM figures have improved (initially were around 129% in all the cases of study) and the spectral regrowth has been corrected (see Fig. 7 and ACPR values in Table I). However, these figures are slightly worse when using the HEA because nonlinear distortions are bigger and more difficult to compensate. It was found

TABLE I

Measure	$V_{DD}(t) = E(t)$		$V_{DD}(t) = E_{BWR}(t)$	
	LEA	HEA	LEA	HEA
BW_{VDD} [MHz]	30	30	2	2
$PAPR_{VDD}$ [dB]	7.17	7.17	5.03	5.03
P_{out} LEA [W]	1.37	0.55	2.5	0.41
P_{RFout} [W]	0.59	0.58	0.63	0.65
η_{LEA} [%]	37	57	49	59
η_{EA} [%]	37	77	49	83
η_{ET} [%]	15	22	12	20
$ACPR_L$ [dB]	-61	-60.54	-60.65	-60.80
$ACPR_U$ [dB]	-61	-60.45	-60.73	-60.75
EVM [%]	0.89	1.38	0.98	1.01

that, in general, the larger the RF BW's signal is, the more difficult to compensate are the nonlinear distortions associated to the envelope. As a counterpart, the LEA might need to compensate high frequency components and therefore need a larger frequency response. Nevertheless, the BW requirements are lower than when only LEA is considered.

V. CONCLUSION

As it has been experimentally shown, the RFPA efficiency is degraded as the SR and BW reduction of the envelope increases. However, since switched amplifiers are more efficient at low frequency bands, this efficiency degradation could be compensated by having better efficiency figures at the EA stage. Such approach is brought into practice by the HEA. The experimental results have shown that the proposed EA improves the efficiency of the ET while keeping high linearity figures. As expected, the best efficiency figures are obtained when using the HEA and the RF envelope signal supplies the RFPA. However for wide band signals is not always possible to perform the amplification of its envelope, hence it is necessary to use the BWRE which yield competitive efficiency figures.

ACKNOWLEDGMENT

This work was supported by Spanish Government under project TEC2011-29126-C03-02.

REFERENCES

- [1] F. Raab, "Split-band modulator for Kahn-technique transmitters," in *Microwave Symposium Digest, 2004 IEEE MTT-S International*, vol. 2, June 2004, pp. 887 – 890 Vol.2.
- [2] T. Kato, Y. Funahashi, A. Yamaoka, K. Yamaguchi, J. Zhou, K. Morris, and G. Watkins, "Performance of a frequency compensated EER-PA with memoryless DPD," in *Microwave Conference Proceedings (APMC), 2010 Asia-Pacific*, Dec. 2010, pp. 9 –12.
- [3] G. Montoro, P. Gilabert, E. Bertran, and J. Berenguer, "A method for real-time generation of slew-rate limited envelopes in envelope tracking transmitters," in *RF Front-ends for Software Defined and Cognitive Radio Solutions (IMWS), 2010 IEEE International Microwave Workshop Series on*, Feb. 2010, pp. 1 –4.
- [4] J. Jeong, D. Kimball, M. Kwak, C. Hsia, P. Draxler, and P. Asbeck, "Wideband envelope tracking power amplifiers with reduced bandwidth power supply waveforms and adaptive digital predistortion techniques," *Microwave Theory and Techniques, IEEE Transactions on*, vol. 57, no. 12, pp. 3307 –3314, Dec. 2009.
- [5] P. L. Gilabert and G. Montoro, "Look-up table implementation of a slow envelope dependent digital predistorter for envelope tracking power amplifiers," *Microwave and Wireless Components Letters, IEEE*, vol. 22, no. 2, pp. 97 –99, Feb. 2012.